Published in final edited form as:
Aging Cell. 2012 August ; 11(4): 704–713. doi:10.1111/j.1474-9726.2012.00838.x.

Impairment of Osteoblast Differentiation Due to Proliferation-independent Telomere Dysfunction in Mouse Models of Accelerated Aging

Haitao Wang[1], **Qijun Chen**[2], **Seoung-Hoon Lee**[3], **Yongwon Choi**[2], **F. Brad Johnson**[2], and **Robert J. Pignolo**[1,4]

[1]Department of Orthopaedic Surgery, Perelman School of Medicine, University of Pennsylvania, Philadelphia, PA 19104

[2]Department of Pathology and Laboratory Medicine, Perelman School of Medicine, University of Pennsylvania, Philadelphia, PA 19104

[3]Institute of Biomaterials, Department of Oral Microbiology and Immunology, Wonkwang University School of Dentistry, Iksan 570-749, Republic of Korea

[4]Department of Medicine, Perelman School of Medicine, University of Pennsylvania, Philadelphia, PA 19104

SUMMARY

We undertook genetic and non-genetic approaches to investigate the relationship between telomere maintenance and osteoblast differentiation, as well as to uncover a possible link between a known mediator of cellular aging and senile bone loss. Using mouse models of disrupted telomere maintenance molecules, including mutants in the Werner helicase ($Wrn^{-/-}$), telomerase ($Terc^{-/-}$) and $Wrn^{-/-}$ $Terc^{-/-}$ double mutants predisposed to accelerated bone loss, we measured telomere dysfunction-induced foci (TIFs) and markers of osteoblast differentiation in mesenchymal progenitor cells (MPCs). We found that telomere maintenance is directly and significantly related to osteoblast differentiation, with dysfunctional telomeres associated with impaired differentiation independent of proliferation state. Telomere-mediated defects in osteoblast differentiation are associated with increased p53/p21 expression and concomitant reduction in RUNX2. Conversely, MPCs from $p53^{-/-}$ mice do not have substantial telomere dysfunction and spontaneously differentiate into osteoblasts. These results suggest critical telomere dysfunction may be a prominent mechanism for age-related osteoporosis and limits MPC differentiation into bone-forming cells via the p53/p21 pathway.

Corresponding Author: Robert J. Pignolo, M.D., Ph.D., Departments of Medicine and Orthopaedic Surgery, Perelman School of Medicine, University of Pennsylvania, 424B Stemmler Hall, 36th Street and Hamilton Walk, Philadelphia, PA 19104, Telephone: 215-746-8138; FAX: 215-573-2133, pignolo@mail.med.upenn.edu.

AUTHOR CONTRIBUTIONS

Haitao Wang: collection and/or assembly of data; data analysis and interpretation; manuscript writing; final approval of manuscript.
Qijun Chen: provision of study materials; final approval of manuscript.
Seoung-Hoon Lee: collection and/or assembly of data; data analysis and interpretation; manuscript writing; final approval of manuscript.
Youngwon Choi: data analysis and interpretation; manuscript writing; final approval of manuscript.
F. Brad Johnson: provision of study materials; data analysis and interpretation; manuscript writing; final approval of manuscript.
Robert J. Pignolo: conception and design; financial support; collection and/or assembly of data; data analysis and interpretation; manuscript writing; final approval of manuscript.

Keywords

Telomere; telomere dysfunction; aging; osteoporosis; mesenchymal stem cells

INTRODUCTION

The uncoupling of bone formation from bone resorption leads to a net loss of bone and an increase in skeletal fragility, the major hallmarks of osteoporosis. In general terms, age-related bone loss is characterized predominantly by reduced bone formation (secondary to decreased osteoblast number and activity) in the setting of persistent bone resorption (Kassem & Marie, 2011; Marie & Kassem, 2011). In contrast, post-menopausal osteoporosis leads primarily to an increase in osteoclast-mediated accelerated bone resorption (Kassem & Marie, 2011; Marie & Kassem, 2011).

Previously we and others found that deficiency in telomerase (TERC), alone or in combination with another genome maintenance enzyme, the Werner helicase (WRN), leads to a low bone mass phenotype in older animals (Chang et al., 2004; Du et al., 2004; Pignolo et al., 2008; Saeed et al., 2011). Impairment in osteogenic potential (decreased mesenchymal progenitor cells or MPCs) and osteoblast differentiation (decreased expression of osteoblast markers) are the major cellular mechanisms involved in premature bone loss (Pignolo et al., 2008). In older animals, osteoclast number and in vitro differentiation in $Wrn^{-/-}$, $Terc^{-/-}$ and $Wrn^{-/-}Terc^{-/-}$ mutants are comparable to those in age-matched wild-type mice (Pignolo et al., 2008). MPCs derived from these mutant genotypes have a shortened in vitro life span concomitant with reduced osteogenic potential and osteoblast differentiation.

The association between age-related bone loss and stem cell defects in the aged animal may likely be related to proliferative decline in MPCs, suggesting that replicative senescence is perhaps a causative etiology for limited stem cell pools and impaired differentiation into bone-forming cells (Gronthos et al., 2003; Pignolo et al., 2008; Shi et al., 2002; Simonsen et al., 2002; Yudoh et al., 2001). Telomere shortening and/or telomere uncapping may then account for both limited replicative capacity and reduced osteoblast differentiation. However, it is also possible that dysfunctional telomeres limit proliferation and differentiation as mutually exclusive events or set differential thresholds for impairments in proliferation and differentiation.

Here we take genetic and non-genetic approaches to explore the possibility that telomere-based mechanism(s) influence the robustness of osteoblast differentiation. We show that in young animals telomerase deficiency and accelerated telomere shortening can impair osteoblast differentiation through a p53/p21 mechanism. Unexpectedly, we found that telomere dysfunction limits MPC number and osteoblast differentiation independent of cell proliferation state. Conversely, telomere maintenance by low oxygen tension or reduced telomere attrition preserves MPC number and ability to differentiate into bone-forming cells.

RESULTS

Impairment in osteoblast differentiation but not osteoclast differentiation or function occurs with telomerase deficiency

We previously demonstrated that osteoclast number and differentiation were preserved in old $Wrn^{-/-}$ and $Terc^{-/-}$ mutants, as well as in $Wrn^{-/-}Terc^{-/-}$ mutants compared to wild-type mice (Pignolo et al., 2008), indicating the major cellular mechanism for age-related osteoporosis was impaired osteoblast differentiation and function. In the current study, using young (3 month old) animals from all mutant genotypes, we confirmed that osteoclast

differentiation is also comparable to age-matched wild-type controls (Supporting Information, Fig. S1), although there was a non-statistically significant difference between the $Wrn^{-/-}Terc^{-/-}$ mutants compared to the other genotypes ($p = 0.0390$). We further demonstrated that bone resorption does not categorically change among genotypes (Supporting Information, Fig. S1).

Early passage MPCs derived from young $Terc^{-/-}$ and $Wrn^{-/-}Terc^{-/-}$ mutants undergo reduced osteoblast differentiation, as assessed by expression of osteocalcin and alkaline phosphatase, as well as mineralization of extracellular matrix (Supporting Information, Fig. S2 and Fig. S3, 21% O_2).

Telomere dysfunction, independent of cell proliferation state, limits MPC number and osteoblast differentiation

In order to study the role of telomere-based mechanisms for impaired osteoblast differentiation that accompanies age-related bone loss, we evaluated mesenchymal progenitor cells (MPCs) derived from 3 month old $Wrn^{-/-}$ and $Terc^{-/-}$ single mutants, as well as in $Wrn^{-/-}Terc^{-/-}$ double mutants. Disruption of telomere maintenance molecules such as WRN and TERC, either alone or in combination, shorten the in vitro life span of MPCs (Supporting Information, Fig. S4). Through the fourth in vitro passage, however, there were no statistically significant differences in the change in population doublings between wild-type MPCs and those derived from mutant animals (Supporting Information, Fig. S4). Therefore, in order to control for the effect of telomere-based proliferation defects on osteoblast differentiation, we conducted all experiments at the first in vitro passage, when there were also no statistically significant differences among genotypes in the incorporation of BrdU into dividing MPCs ($p > 0.05$) or in apoptotic cell death ($p > 0.05$).

We analyzed telomere length in MPCs and found that there was a statistically significant shortening in the $Terc^{-/-}$ and $Wrn^{-/-}Terc^{-/-}$ genotypes compared to wild-type (Supporting Information, Fig. S5). No difference in telomere length was observed between $Terc^{-/-}$ and $Wrn^{-/-}Terc^{-/-}$ mutants.

Although there was a statistically significant correlation of telomere length with proliferative capacity ($r = 0.87$; $p < 0.001$; $n = 6$), there was not a significant correlation with differentiation ($r = 0.559$; $p > 0.1$; $n = 6$). Since there was no association between the telomere lengths of MPCs from individual animals and their ability to differentiate into bone-forming cells, we quantified telomere dysfunction-induced foci (TIFs), i.e., the co-localization of DNA damage factor(s) with telomeric DNA, as a more sensitive measure of telomere dysfunction. Figure 1 demonstrates the increase in TIFs among MPC nuclei derived from $Terc^{-/-}$ and $Wrn^{-/-}Terc^{-/-}$ mutants. There were few TIFs among MPC nuclei derived from wild-type and $Wrn^{-/-}$ animals.

As many as about 70% of MPCs from 3 month old $Wrn^{-/-}$ $Terc^{-/-}$ double mutants were found to have dysfunctional telomeres, with stem cell colony-forming units (CFU-F) and alkaline phosphatase positive CFU (CFU-AP) reaching only approximately 26% and 22% of wild-type levels, respectively (Fig. 1B). MPCs from wild-type and $Wrn^{-/-}$ single mutants had low levels of telomere dysfunction and intact Ob differentiation, while MPCs from $Terc^{-/-}$ mutants had levels of telomerase dysfunction and Ob differentiation capacity in between those derived from wild-type and the double mutant mice (Fig. 1B). MPCs derived from $Terc^{-/-}$ and $Wrn^{-/-}Terc^{-/-}$ mutants also had statistically significantly more TIFs per cell compared to those derived from wild-type or $Wrn^{-/-}$ mutants ($p < 0.005$).

The number of colony-forming units-fibroblast (CFU-F), taken to indicate MPC abundance, was significantly negatively correlated ($p < 0.04$) with the percentage of MPC nuclei

containing dysfunctional telomeres (Fig. 1B). The number of colony-forming units-alkaline phosphatase (CFU-AP), taken to indicate MPC osteoblast differentiation, was also significantly negatively correlated ($p < 0.02$) with the percentage of MPC nuclei containing dysfunctional telomeres (Fig. 1B). In biological systems, r_F and r_{AP} values of 0.54 and 0.77, respectively, represent good to very good relationships, with 29% of the variation in CFU-F and 59% of the variation in CFU-AP being accounted for by telomere dysfunction. There was a statistically significant correlation between TIFs and telomere length ($r= 0.98$; $p<0.001$; $n=10$), but as mentioned above, no statistically significant correlation between telomere length and osteoblast differentiation.

Telomere maintenance by low oxygen tension or limiting telomeric attrition preserves MPC number and osteoblast differentiation

We undertook additional approaches to independently test the hypothesis that telomere dysfunction is related to age-related impairment in osteoblast differentiation. We subjected MPCs to low oxygen tension (to reduce genotoxic stress and minimize telomere dysfunction), and again assayed for TIFs and markers of Ob differentiation.

MPCs appropriately respond to reduced oxygen tension (1% O_2) by enacting nuclear translocation of transcription factor HIF1-α (Supporting Information, Fig. S6). Low oxygen limited telomere dysfunction and significantly enhanced Ob differentiation. Low O_2 decreased the number of dysfunctional telomeres in MPCs from $Wrn^{-/-}$ $Terc^{-/-}$ mutants by about 41% (Fig. 2A), with concomitant increases in osteocalcin expression (Supporting Information, Fig. S2), in alkaline phosphatase activity and mineralization (Supporting Information, Fig. S3), and in CFU-F as well as CFU-AP number (Fig. 2B–C). The effect of low oxygen tension in promoting Ob differentiation of MPCs was statistically significant in those isolated from $Terc^{-/-}$ and $Wrn^{-/-}$ $Terc^{-/-}$ mutants, where the percentages of dysfunctional telomeres were the highest.

We also evaluated the effects of limited telomere attrition on the number of TIFs and concomitant measures of osteoblast differentiation by comparing MPCs derived from forth generation (G4) and first generation (G1) $Terc^{-/-}$ animals. G1 $Terc^{-/-}$ mice have reduced TIFs (Fig. 3A–B) and preserved measures of osteoblast differentiation, including alkaline phosphatase activity and mineralization (Fig. 3C), osteocalcin expression (Fig. 3D) and CFU-AP number (Fig. 3E), compared to G4 $Terc^{-/-}$ animals. These findings also indicate that telomerase deficiency, *per se*, does not explain the Ob defects, but rather that they are caused by telomere dysfunction.

The p53/p21 pathway regulates osteoblast differentiation in telomere-mediated MPC aging

The tumor suppressor p53 has been proposed as a negative regulator of osteoblast differentiation (Lengner et al., 2006; Wang et al., 2006); however, it is unclear if p53 plays a role in telomere-mediated impairment of osteoblastogenesis with MPC aging. Differentiated MPCs derived from $Wrn^{-/-}$ $Terc^{-/-}$ mutants upregulate p53 and the downstream cell-cycle cyclin-dependent kinase inhibitor, p21 (Fig. 4). While the master osteoblast transcriptional regulator Runx2 is robustly expressed in differentiating MPCs derived from wild-type mice, it is suppressed in differentiating MPCs derived from $Wrn^{-/-}Terc^{-/-}$ mice (Fig. 4).

To further evaluate the relationship between p53 and telomere maintenance during differentiation into bone-forming cells, we analyzed TIF formation and measures of osteoblast differentiation in MPCs derived from $p53^{-/-}$ mice. Both using early and later passage $p53^{-/-}$ MPCs, the number of TIF+ cells were comparable to those from wild-type animals (Fig. 5A–B). Osteoblast differentiation, as measured by alkaline phosphatase activity, mineralization, and osteocalcin expression occurred spontaneously (in the absence

of differentiation factors) in $p53^{-/-}$ MPCs (Fig. 5C–D). The numbers of CFU-F and CFU-AP were greater in $p53^{-/-}$ MPCs (beginning at the sixth passage and continuing through to passage 22) compared to wild-type MPCs (Fig. 5E).

DISCUSSION

Human age-related bone loss is primarily due to declines in osteoblast differentiation and function (Kassem & Marie, 2011; Marie & Kassem, 2011). In the $Wrn^{-/-}Terc^{-/-}$ model of acclerated aging, the osteoporotic phenotype of these mice is also associated with a major decline in osteoblast differentiation and function (Pignolo et al., 2008). In young and older animals, osteoclast differentiation of isolated bone marrow mononuclear cells and osteoclast function are intact across genotypes with defective telomere maintenance molecules (including $Wrn^{-/-}$, $Terc^{-/-}$, and $Wrn^{-/-}Terc^{-/-}$), and comparable to age-matched wild-type mice (this paper and (Pignolo et al., 2008)). However, increased osteoclast number and size was recently reported in $Terc^{-/-}$ mice by bone histomorphometry, and serum obtained from these mice promoted osteoclast formation of wild-type bone marrow cultures (Saeed et al., 2011). These correlative findings support that dysfunctional telomere-based mouse models may recapitulate primary and secondary mechanism(s) of senile bone loss, with dysfunctional telomeres as the putative basis for defects in bone-forming cells and their precursors, as well as for an inflammatory microenvironment that enhances osteoclast formation in vivo.

Here we focused on uncovering telomere-based mechanisms for defective osteoblast differentiation. Using genetic and non-genetic approaches, we showed that telomere maintenance is required for adequate osteoblast differentiation (Fig. 6). Telomere dysfunction impairs osteoblast differentiation as well as reduces proliferative capacity. Although senescence of MPCs is associated with reduced ability to differentiate into bone-forming cells (Kretlow et al., 2008; Zhou et al., 2008), telomere dysfunction appears to abrogate osteoblast differentiation independently of MPC proliferative state (Fig. 6). By using early passage MPCs from wild-type and mutant genotypes that are proliferatively indistinguishable, we showed that MPCs lose the ability to differentiate before they become replicatively senescent. This is consistent with the idea that differentiation is a process much more sensitive to telomere maintenance than is proliferation; that is, the threshold for telomeric damage may be lower with differentiation compared to proliferation. Thus, our data suggests that dysfunctional telomeres may limit proliferation and differentiation as mutually exclusive events.

Although WRN interacts with several proteins critical for telomere function, occasionally localizes to nuclear foci containing telomere DNA, and has clear functional roles in the replication of telomeres in human cells lacking telomerase (Yankiwski et al., 2000; Johnson et al., 2001; Opresko et al., 2002; Crabbe et al., 2004), our previous and current data indicate that deficits of MPCs derived from $Wrn^{-/-}$ mice are minimal and may act to negatively synergize with telomerase deficiency only slightly. One possible explanation is that there are species-specific differences in the function of WRN as a genome maintenance molecule. Another possible explanation is that under conditions where the effects of replicative senescence are minimized and telomerase is intact, osteoblast differentiation in $Wrn^{-/-}$ MPCs is relatively unaffected.

Threshold effects of dysfunctional telomeres are also suggested by the role of DNA damage responses in the initiation and suppression of tumorigenesis (Cosme-Blanco & Chang, 2008). Dose-dependent telomeric instability in response to radiation also supports the importance of threshold effects (Urushibara et al., 2004). While it is clear that telomeres which have uncapped due to critical shortening or other perturbations in telomere structure

(e.g., loss of shelterin components) generate DNA damage signals, it is not clear that the particular signals are identical in all cases with regard to the actions of suppressor genes that limit the expansion of damaged cells (e.g., p53).

However, there is a growing body of evidence that suggests p53 is a negative regulator of osteoblast differentiation (Lengner et al., 2006; Wang et al., 2006). We demonstrated here that p53 mediates telomere-based impairment of osteoblastogenesis with MPC aging; in fact, MPCs from $p53^{-/-}$ mice show minimal telomere dysfunction relative to wild-type and undergo spontaneous osteoblast differentiation. The cell-cycle cyclin-dependent kinase inhibitor p21, which functions downstream of p53, is markedly up-regulated while the requisite obteoblast transcription factor RUNX2 is suppressed in differentiating MPCs derived from $Wrn^{-/-}$ $Terc^{-/-}$ mice. That p21 may be an effector of impaired osteoblast differentiation due to dysfunctional telomeres (Fig. 6) is also supported by its role as a mediator of fibroblast growth factor inhibition of osteoblast differentiation (Bellosta et al., 2003). Thus, there is a clear relationship between p53 signaling and osteoblast differentiation in two different models, one where increased p21 expression is associated with decreased Runx2 expression and concomitant impaired differentiation ($Wrn^{-/-}$ $Terc^{-/-}$ double mutant mouse model), and one where knock out of p53 causes spontaneous osteoblast differentiation ($p53^{-/-}$ mouse model). In each model, p53 signaling is inversely related to telomere maintenance and the efficiency of osteoblast differentiation, suggesting as least one mechanism by which telomere dysfunction may lead to impaired differentiation.

Declines in osteogenic measures with age have been reported for human and mouse MPCs (Kretlow et al., 2008; Zhou et al., 2008). Although there is insufficient evidence to be certain of the causal roles that telomere dysfunction may play in age-related osteoporosis, there are several indications that it may be of importance. Human bone-marrow derived MPCs do not exhibit telomere lengthening mechanisms (Bernardo et al., 2007). Expression of telomerase in human MSCs extends proliferative capacity in vitro, accelerates their osteogenic differentiation, and enhances bone formation when these MSCs are transplanted into mice (Simonsen et al., 2002; Yudoh et al., 2001). Further, both progeriod syndromes on which the $Wrn^{-/-}$ $Terc^{-/-}$ accelerated aging model is based (Werner syndrome and dyskerostis congenita, respectively) display accelerated osteoporosis (Hofer et al., 2005; Mason et al., 2005).

A dual role for telomere maintenance in differentiation as well as proliferation is emerging. For example, telomere-dependent activation of endothelial cell differentiation and protection against apoptosis has been reported (Zaccagnini et al., 2005). Telomere dysfunction in human keratinocytes elicits senescence as well as upregulation of genes associated with keratinocyte terminal differentiation. Our data suggests that dysfunctional telomeres may limit proliferation and differentiation as mutually exclusive events. Telomerase dysfunction in aging stem cells promotes genomic instability and in the presence of diminished DNA repair mechanisms alters the pattern of both proliferation and differentiation (Kenyon &Gerson, 2007).

Telomere dysfunction, and its effects on osteoblast differentiation, can be minimized by reducing genotoxic stress or limiting the attrition of telomeres. Lowering oxygen tension in MPC cultures derived from $Terc^{-/-}$ and $Wrn^{-/-}Terc^{-/-}$ mice reduces TIFs with concomitant restoration of osteoblast differentiation to near wild-type levels. Reduced oxygen decreases the already low number of wild type MPCs with TIFs, but does not significantly increase measures of osteoblast differentiation. That low oxygen enhances osteoblast differentiation of MPCs would seem to be contradictory to multiple reports (D'Ippolito et al., 2006; Fehrer et al., 2007; Potier et al., 2007; Salim et al., 2004); however, these reports examined MPCs with negligible telomere dysfunction (non-senescent, wild-type cells or cells that are

telomerase-positive). TIF-postive MPCs from G1 $Terc^{-/-}$ mutants are less abundant than those from G4 generation $Terc^{-/-}$ mutants and MPCs from G1 $Terc^{-/-}$ mutants retain the capacity to undergo osteoblast differentiation. Taken together, these results again imply that a threshold for telomeric damage exists, above which osteoblast differentiation becomes adversely affected.

In vivo, MPCs likely exist at partial pressures of oxygen between one and seven percent (Antoniou et al., 2004; Chow et al., 2001; Ishikawa &Ito, 88), and so culture conditions reflecting ambient O_2 do not closely mimic those found in bone tissue. However, studying osteoblast differentiation at differing oxygen tensions provides valuable insight into the susceptibility of MPCs to stressful conditions that occur with aging and how they respond to such stresses. It has been suggested that replicative capacity in culture is an indirect measure of cellular sensitivity to stress (Campisi & d'Adda di Fagagna, 2007). Using disparate oxygen tensions, our data indicates that telomere dysfunction is a direct measure of cellular sensitivity to genotoxic stress, and with physiologically relevant effects on age-related skeletal pathology.

Just as senescence-associated growth arrest is accompanied by changes in cell phenotype (Campisi & d'Adda di Fagagna, 2007), so too may telomere dysfunction; in this case, failure of MPCs to take on an osteogenic phenotype. Gradual accumulation of senescent cells may in part explain some age-related declines in tissue structure and function (Funk et al., 2000; Parrinello et al., 2005). Our data would also suggest that the accumulation of cells with telomere dysfunction, as a precursor to or independent of senescence, or in response to stress, also contributes to alterations in skeletal structure with adverse functional consequences such as osteoporosis.

EXPERIMENTAL PROCEDURES

Animals

The University of Pennsylvania Institutional Animal Care and Use Committee (IACUC) approved the use of mice described in this paper. Mutant mice had the Wrn and Terc alleles backcrossed onto the C57Bl/6 background (for > 11 generations). G4 $Terc^{-/-}$ and G4 $Wrn^{-/-}$ $Terc^{-/-}$ mice were generated as follows: $Wrn^{+/-}$ $Terc^{+/-}$ mice were crossed to generate G1 $Wrn^{+/-}$ $Terc^{-/-}$ mice. These were in turn bred to generate G2 and G3 $Wrn^{+/-}Terc^{-/-}$ mice, which were used to generate G4 $Wrn^{+/+}$ $Terc^{-/-}$ and G4 $Wrn^{-/-}$ $Terc^{-/-}$ mutants. Cousin matings were used throughout to avoid generation of substrains that can be caused by stochastic differences in telomere length in individual mice. Wild type mice were obtained via standard matings using the C57Bl/6 strain that was used for backcrossing the Wrn and Terc alleles. $Wrn^{-/-}$ mutants were generated by crossing $Wrn^{+/-}$mutants. $Terc^{-/-}$ and $Wrn^{-/-}Terc^{-/-}$ mice used in experiments were from G4 lineages. $P53^{-/-}$mice used in experiments have been previously described (Jacks et al., 94). Three-month male old mice from each genotype were used in experiments. Unless otherwise stated, four animals from each genotype were used for each experiment.

Isolation of Mesenchymal Progenitor Cells (MPCs)

Soft tissue was removed along the femoral shaft and metaphyses were removed. Bone marrow plugs were expelled by insertion of a 21 gauge needle into the marrow cavity and flushing the cavity with 10 ml of α-Minimal Essential Medium (α-MEM) with nucleosides (Gibco/Invitrogen). The bone marrow cells (marrow plugs) from femurs of the same aminal were collected, pooled, and dispersed by repeat pipeting before centrifugation at 1000 × g for 10 minutes. The supernatant was removed and the pellet resuspended in α-MEM containing 10% fetal calf serum (FCS, Hyclone). Cells were plated at a density of two

marrow plugs per 25 cm^2 of tissue culture growth surface and refed every three days until confluent. Cell strains were derived from individual animals.

Cell Culture, Determination of Replicative Life Span, and BrdU Incorporation

MPCs were cultured in α-MEM with nucleosides plus 10% FCS. For life span studies, cells were seeded at a density of 1×10^4 cells/cm^2 at each passage and grown until confluent, usually by 10 days (Cristofalo &Charpentier, 1980). Cultures were defined as being at the end of their proliferative lifespan when they were unable to complete one population doubling during a 2-week period. For experiments performed under low oxygen conditions (1% O_2), cell culture vessels were placed in hypoxia chambers (Billups-Rothenberg Inc., CA).

For bromodeoxyuridine (BrdU) labeling, MPCs were grown on glass coverslips and a 1:1000 ratio of BrdU solution (Invitrogen) was added to culture plates during the log phase of growth (day 3 after seeding) and incubated for 24 hours. Cells were washed three times with sterile PBS, fixed with 2 % paraformaldehyde containing Triton X-100 for 30 minutes, and incubated with a 1:500 dilution of anti-BrdU (Invitrogen) for 2 hours. DAPI was then added at a dilution of 1:500 for 1min. At least 100 cells per sample were scored in randomly selected fields under fluorescence microscopy.

Measurement of Apoptosis

Apoptosis was assessed using the TUNEL assay kit TACS•XL® DAB In Situ Apoptosis Detection (Trevigen, Inc, Gaithersburg, MD) according to the manufacturer's instructions.

Osteoblast Differentiation

MPC cultures were seeded at 2×10^4 cell/cm^2 and refed three times weekly with α-MEM + 10% FCS +/− 50μg/ml ascorbic acid (Sigma Chemical Co.), 10mM β-glycerophosphate (Sigma Chemical Co.), and 10 nM dexamethasone (Sigma Chemical Co.). Media containing differentiation factors was replaced at regular intervals until mineralization was detected, usually within 2–4 weeks. Each culture was derived from MPCs pooled from the femurs of the same animal. CFU-F (taken to indicate MPC abundance) and CFU-AP (taken to indicate MPC osteoblast differentiation) were quantitated by light microscopy as the number of colonies containing at least 10 cells at the same time in vitro when parallel wild-type cultures demonstrated evidence of mineralization. The number of colonies was quantitated using Image J software (http://rsb.info.nih.gov/ij/).

Osteoclast Differentiation and Bone Resorption Assay

Twenty-four hours after plating marrow plugs, non-adherent bone marrow (BM) cells were removed from the same cultures used to derive MPC strains. Murine osteoclasts were prepared from bone marrow cells as described previously (Lee et al., 2008). In brief, 1×10^7 BM cells were cultured with α-MEM/10% FCS with M-CSF (30 ng/ml) using Corning 100mm non-tissue culture-treated dishes (Corning Incorporated Life Science, Acton, MA). After 3 days of culture, floatingcells were removed and attached bone-marrow-derived macrophages (BMMs) used as osteoclastprecursors. To generate osteoclasts, BMMs were cultured with TRANCE (150 ng/ml) and M-CSF (30 ng/ml) in 96-well culture plates (Corning; 1×10^4 cells/0.2 ml/well). After 3 days of culture, the medium was changed with fresh α-MEM/10% FCS containing TRANCE (150 ng/ml) and M-CSF (30 ng/ml), and cultured for one day more. After cells were washed in PBS, and fixed in 10% formalin, they were stained for TRAP (tartrate-resistant acid phosphatase) in the presence of 0.05M sodium tartrate (Sigma Chemical Co.). The substrate used was naphthol AS-MX phosphate (Sigma Chemical Co.). TRAP+ cells containing more than 3 nuclei were considered to be

osteoclasts. Visualization of images was performed using a Nikon Diaphot 300 microscopy and an inverted, 10x/0.25na Ph1 DL objective. Images were captured using a Hamamatsu C8484-05G CCD camera and Adobe Photoshop software.

Bone resorption assays were performed as described (Lee et al., 2008). Briefly, BMMs were loaded onto dentine slices and cultured in the presence of M-CSF (30 ng/ml) and TRANCE (150 ng/ml) for 4 days. The slices were then recovered, cleaned by ultrasonication in 0.5 M NH_4OH to remove adherent cells. To visualize resorption pits, dentine slices were stained with 0.5% toluidine blue (Sigma). Microscopy and image capture were performed as for osteoclast differentiation.

Immunofluorescence studies

Adherent cells grown on glass coverslips to about 60% confluence were washed twice with 1X phosphate-buffered saline (PBS) and fixed with 2 % paraformaldehyde containing Triton X-100 for 30 minutes. After rinsing with PBS, cells were placed in blocking solution containing 1% bovine serum albumin (BSA) in PBS for 30 minutes. Primary antibodies against HIF1α (Novus Biological, CO) or osteocalcin (Santa Cruz Biotechnology, Santa Cruz, CA) were diluted 1:600 and 1:500, respectively, based on the manufacturer's recommendation and experience from previous use, and incubated with cells in a humidified container for 2 hours. Unbound primary antibody was washed out with three rinses of PBS before incubation of cells with fluorescently-tagged Alexa-fluor 594 (1:1000 dilution) or Alexa-fluor 488 (Invitrogen) secondary antibodies, respectively. DAPI was added at a dilution of 1:500 for 1min. After rinsing cells three times with PBS, coverslips were mounted onto slides. All steps were performed at room temperature. Preimmune serum was used as a negative control at a dilution comparable to that of the primary antibody. All dilutions were made in blocking solution. Slides were stored at 4°C in the dark. Cells were visualized using a Nikon Eclipse TE2000-U fluorescence microscope and Nikon Plan Fluor 10X0.30 and 20X0.45 objectives. Image capture was performed using NIS Elements Imaging Software 3.10 Sp2 and a Photometrics Coolsnap EZ camera.

Histology

A specific alkaline phosphatase substrate 5-bromo-4-chloro-3-indolyl-phosphate (BCIP, Moss, Inc., Maryland, USA) in the presence of p-nitro blue tetrazolium chloride (NBT) was used to detect alkaline phosphatase activity (cells are stained blue/purple). Alizarin red S staining was used to detect a mineralized matrix. Crystal violet staining was used to detect CFU-F. Color images of tissue culture plates containing stained cells were captured using an Epson Perfection 4490 scanner set at a resolution of 1200 dpi.

Western Blot Analysis

Total protein was lysed in RIPA buffer (150 mM NaCl, 1.0% IGEPAL® CA-630, 0.5% sodium deoxycholate, 0.1% SDS, 50 mM Tris, pH 8.0.)[Sigma, St. Louis, MO] with 1× protease inhibitor cocktail (Sigma, St. Louis, MO) and phosphatase inhibitor cocktail (Thermo Scientific, Rockford, IL). The lysate was incubated on ice for 15 min and centrifuged at 12,000 g for 10min. Protein in the supernatant was quantified using the BCA Protein Assay kit (Thermo Scientific, Rockford, IL). Twenty micrograms of total protein were separated on a 10% SDS-PAGE gel and then transferred to nitrocellulose membranes (Invitrogen, Carlsbad, CA) by electroblotting. Membranes were incubated overnight at 4°C with a 1:1000 dilution of antibody specific for P53 (Abcam, Cambridge, MA), P21 (Santa Cruz, Santa Cruz, CA.), Runx2 (Abcam, Cambridge, MA) or β-actin (Santa Cruz, Santa Cruz, CA.) in PBS containing 5% nonfat milk or 5% BSA. Membranes were washed with PBST (0.1%Tween-20) and incubated for 1 h with the corresponding secondary antibody conjugated with horseradish peroxidase. An enhanced ECL chemiluminescent Western

blotting detection system Millipore (Billerica, MA) was used to detect the antigen-antibody complex. Image capture was performed using an Epson Perfection 4490 scanner set at a resolution of 300 dpi. The bands were quantified using NIH Image J software (http://rsb.info.nih.gov/ij/).

Genomic DNA Isolation, Southern Blotting, and Quantitation of Telomere Length

DNA plugs for contourclamped homogeneous electric field (CHEF) gel electrophoresis were prepared as described [(Gerring et al., 1991); Bio-Rad CHEF-DR II system instruction manual]. DNA embedded in agarose plugs was digested with Dpn II and electrophoresed through 1% agarose gels in 0.5× TBE maintained at 4°C, using a CHEF DR-II pulsed-field apparatus (Bio-Rad). Separation was for 24 hr at 6 V/cm at a constant pulse time of 5 s. The gel was dried at 50°C for 1 hour and hybridized with a ^{32}P-γATP-labeled $(CCCTAA)_4$ probe. The gel was then washed 3 × 20 minutes in 4X SSC at room temperature and 3 × 20 minutes in 4X SSC, 0.1%SDS at 57°C. Image scanning was performed using a Typhoon 9200 phosphoimager (GE Healthcare) at 200 μm resolution. The mean telomere length (MTL) was determined by averaging the signal intensity along the telomeric smear (Image J software, http://rsb.info.nih.gov/ij/) as a function of DNA length determined by migration distance compared to molecular weight standards on the same blot (Kimura et al., 2010).

Telomere dysfunction-induced foci (TIF) Assay

Paraformaldehyde fixed MPCs were stained by telomere FISH using a 5ug/ml Cy3-conjugated peptide nucleic acid (PNA) probe specific to the telomere repeat TTAGGG (Panagene Inc, Korea) and modifications to previously described methods (Hao et al., 2004; Herbig et al., 2004). Cells at near-confluency were replated onto glass slides and grown overnight to maintain near-confluency, then washed in PBS for 1 minute before fixing in 4% paraformaldehyde for 10 minutes at room temperature. Cells were permeabilized in 0.2% Triton X-100 in PBS for 1 minute and then washed once in PBS, both at room temperature. Cells were incubated with 4% BSA blocking solution (PBS containing 0.2% Tween, 4% BSA, and 0.02% azide) for 30 minutes at 37°C in a humid chamber. After removal of blocking solution, antibody to 53BP1 (Molecular Probes anti-53BP1 rabbit polyclonal) or γH2AX (Upstate γH2AX mouse monoclonal) was incubated with cells at a 1:1000 dilution in 1% BSA blocking solution (PBS with 1% BSA, 0.2% Tween, and 0.02% azide) for 2 hours at 37°C in a humid chamber. After three 5-minute washes in PBS with 0.2% Tween, Alexa-Fluor 488 conjugated goat anti-rabbit (1:500 dilution in PBS with 1% BSA, 0.2% Tween, and 0.02% azide) or Alexa-Fluor 488 conjugated goat anti-mouse (1:500 dilution in PBS with 1% BSA, 0.2% Tween, and 0.02% azide) was incubated for 1 hour at 37°C in a humid chamber. After another three 5-minute washes in PBS with 0.2% Tween, incubation in 4% paraformaldehyde for 20 minutes, and washing in 0.25M glycine for 10 minutes, serial dehydration steps in 70%, 90%, and 100% ethanol were performed for three minutes each. Hybridization solution containing 0.5 μg/ml Cy3 PNA probe, 70% freshly deionized formamide, 2.5 mg/ml acetylated BSA, 12 mM Tris-HCl (pH 8), 4.95 mM KCl, 1mM $MgCl_2$, and 0.001% Triton X-100 was added to each slide overlaid with a glass coverslip before denaturization at 83°C for 4 minutes. Hybridization in a humid chamber proceeded for 18 hours in the dark. After removal of coverslips, three 10-minute washes in 70% formamide/2X SSC (1X SSC contains 150 mM NaCl, 15mM sodium citrate) were performed. After consecutive washes in 2X SSC and PBS, each for ten minutes, cells were incubated with 1% BSA blocking solution for 30 minutes at 37°C in a humid chamber. Following aspiration of blocking solution, Alexa-488-congugated donkey anti-goat antibody (Invitrogen) at a 1:500 dilution in 1% BSA blocking solution was incubated for 1 hour at 37°C in a humid chamber. Slides were washed sequentially with PBS/0.2% Tween, PBS/0.2% Tween with 0.2 μg/ml DAPI, and PBS/Tween, each for 5 minutes with protection from light. At least 100 nuclei were examined for each sample, and the number of TIFs

(telomere and 53BP1/γH2AX co-localized foci) was counted. TIF-positive cells were defined as those with at least one TIF. Confocal analysis was performed at the University of Pennsylvania Biomedical Imaging Core on a Zeiss LSM510 META NLO laser scanning confocal microscope using a Plan-Apo 63x/1.4 oil objective. Image capture was performed using Zeiss LSM510 META version 4.2 software.

Statistics

For multiple comparisons to the wild-type group, two-sided, unpaired Student's *t*-tests were used with statistical significance set to $p < 0.008$ (Bonferroni adjustment); otherwise p was set to < 0.05. The *t* test for correlation was used to determine if a statistically significant relationship exists between telomere dysfunction and colony-forming units, proliferative capacity, or telomere length (statistical significance set to $p < 0.05$). All experiments on biological replicates were performed in triplicate. Error bars in all figures indicate standard error of the mean. All statistics were performed by Graphpad software (www.graphpad.com).

Supplementary Material

Refer to Web version on PubMed Central for supplementary material.

Acknowledgments

This work was supported by a National Institutes of Health/National Institute on Aging grant R01AG028873 (R.J.P), a University of Pennsylvania Institute on Aging pilot grant award (R.J.P.) and a Penn Center for Musculoskeletal Disorders pilot grant award (R.J.P.). The authors wish to thank Utz Herbig and John Sedivy for technical advice regarding the use of TIF protocols and Eric Brown for the generous gift of $p53^{-/-}$ mice.

References

Antoniou ES, Sund S, Homsi EN, Challenger LF, Rameshwar P. A theoretical simulation of hematopoietic stem cells during oxygen fluctuations: prediction of bone marrow responses during hemorrhagic shock. Shock. 2004; 22:415–422. [PubMed: 15489633]

Bellosta P, Masramon L, Mansukhani A, Basilico C. p21(WAF1/CIP1) acts as a brake in osteoblast differentiation. J Bone Miner Res. 2003; 18:818–826. [PubMed: 12733720]

Bernardo ME, Zaffaroni N, Novara F, Cometa AM, Avanzini MA, Moretta A, Montagna D, Maccario R, Villa R, Daidone MG, Zuffardi O, Locatelli F. Human bone marrow derived mesenchymal stem cells do not undergo transformation after long-term in vitro culture and do not exhibit telomere maintenance mechanisms. Cancer Res. 2007; 67:9142–9149. [PubMed: 17909019]

Campisi J, d'Adda di Fagagna F. Cellular senescence: when bad things happen to good cells. Nat Rev Mol Cell Biol. 2007; 8:729–740. [PubMed: 17667954]

Chang S, Multani AS, Cabrera NG, Naylor ML, Laud P, Lombard D, Pathak S, Guarente L, DePinho RA. Essential role of limiting telomeres in the pathogenesis of Werner syndrome. Nat Genet. 2004; 36:877–882. [PubMed: 15235603]

Chow DC, Wenning LA, Miller WM, Papoutsakis ET. Modeling pO(2) distributions in the bone marrow hematopoietic compartment. II. Modified Kroghian models. Biophys J. 2001; 81:685–696. [PubMed: 11463617]

Cosme-Blanco W, Chang S. Dual roles of telomere dysfunction in initiation and suppression of tumorigenesis. Exp Cell Res. 2008; 314:1973–1979. [PubMed: 18448098]

Crabbe L, Verdun RE, Haggblom CI, Karlseder J. Defective telomere lagging strand synthesis in cells lacking WRN helicase activity. Science. 2004; 306:1951–1953. [PubMed: 15591207]

Cristofalo VJ, Charpentier R. A standard procedure for cultivating human diploid fibroblastlike cells to study cellular aging. Journal of Tissue Culture Methods. 1980; 6:117–121.

D'Ippolito G, Howard GA, Roos BA, Schiller PC. Sustained stromal stem cell self-renewal and osteoblastic differentiation during aging. Rejuvenation Res. 2006; 9:10–19. [PubMed: 16608390]

Du X, Shen J, Kugan N, Furth EE, Lombard DB, Cheung C, Pak S, Luo G, Pignolo RJ, DePinho RA, Guarente L, Johnson FB. Telomere shortening exposes functions for the mouse Werner and Bloom syndrome genes. Mol Cell Biol. 2004; 24:8437–8446. [PubMed: 15367665]

Fehrer C, Brunauer R, Laschober G, Unterluggauer H, Reitinger S, Kloss F, Gully C, Gassner R, Lepperdinger G. Reduced oxygen tension attenuates differentiation capacity of human mesenchymal stem cells and prolongs their lifespan. Aging Cell. 2007; 6:745–757. [PubMed: 17925003]

Funk WD, Wang CK, Shelton DN, Harley CB, Pagon GD, Hoeffler WK. Telomerase expression restores dermal integrity to in vitro-aged fibroblasts in a reconstituted skin model. Exp Cell Res. 2000; 258:270–278. [PubMed: 10896778]

Gerring SL, Connelly C, Hieter P. Positional mapping of genes by chromosome blotting and chromosome fragmentation. Methods Enzymol. 1991; 194:57–77. [PubMed: 2005810]

Gronthos S, Chen S, Wang CY, Robey PG, Shi S. Telomerase accelerates osteogenesis of bone marrow stromal stem cells by upregulation of CBFA1, osterix, and osteocalcin. J Bone Miner Res. 2003; 18:716–722. [PubMed: 12674332]

Hao LY, Strong MA, Greider CW. Phosphorylation of H2AX at short telomeres in T cells and fibroblasts. J Biol Chem. 2004; 279:45148–45154. [PubMed: 15322096]

Herbig U, Jobling WA, Chen BP, Chen DJ, Sedivy JM. Telomere shortening triggers senescence of human cells through a pathway involving ATM, p53, and p21(CIP1), but not p16(INK4a). Mol Cell. 2004; 14:501–513. [PubMed: 15149599]

Hofer AC, Tran RT, Aziz OZ, Wright W, Novelli G, Shay J, Lewis M. Shared phenotypes among segmental progeroid syndromes suggest underlying pathways of aging. J Gerontol A Biol Sci Med Sci. 2005; 60:10–20. [PubMed: 15741277]

Ishikawa Y, Ito T. Kinetics of hemopoietic stem cells in a hypoxic culture. Eur J Haematol. 1988; 40:126–129. [PubMed: 3278928]

Jacks T, Remington L, Williams BO, Schmitt EM, Halachmi S, Bronson RT, Weinberg RA. Tumor spectrum analysis in p53-mutant mice. Curr Biol. 1994; 4:1–7. [PubMed: 7922305]

Johnson FB, Marciniak RA, McVey M, Stewart SA, Hahn WC, Guarente L. The Saccharomyces cerevisiae WRN homolog Sgs1p participates in telomere maintenance in cells lacking telomerase. EMBO J. 2001; 20:905–913. [PubMed: 11179234]

Kassem M, Marie PJ. Senescence-associated intrinsic mechanisms of osteoblast dysfunctions. Aging Cell. 2011; 10:191–197. [PubMed: 21210937]

Kenyon J, Gerson SL. The role of DNA damage repair in aging of adult stem cells. Nucleic Acids Res. 2007; 35:7557–7565. [PubMed: 18160407]

Kimura M, Stone RC, Hunt SC, Skurnick J, Lu X, Cao X, Harley CB, Aviv A. Measurement of telomere length by the Southern blot analysis of terminal restriction fragment lengths. Nat Protoc. 2010; 5:1596–1607. [PubMed: 21085125]

Kretlow JD, Jin YQ, Liu W, Zhang WJ, Hong TH, Zhou G, Baggett LS, Mikos AG, Cao Y. Donor age and cell passage affects differentiation potential of murine bone marrow-derived stem cells. BMC Cell Biol. 2008; 9:60. [PubMed: 18957087]

Lee SH, Kim T, Jeong D, Kim N, Choi Y. The tec family tyrosine kinase Btk Regulates RANKL-induced osteoclast maturation. J Biol Chem. 2008; 283:11526–11534. [PubMed: 18281276]

Lengner CJ, Steinman HA, Gagnon J, Smith TW, Henderson JE, Kream BE, Stein GS, Lian JB, Jones SN. Osteoblast differentiation and skeletal development are regulated by Mdm2-p53 signaling. J Cell Biol. 2006; 172:909–921. [PubMed: 16533949]

Marie PJ, Kassem M. Extrinsic mechanisms involved in age-related defective bone formation. J Clin Endocrinol Metabol. 2011; 96:600–609.

Mason PJ, Wilson DB, Bessler M. Dyskeratosis congenita -- a disease of dysfunctional telomere maintenance. Curr Mol Med. 2005; 5:159–170. [PubMed: 15974869]

Opresko PL, von Kobbe C, Laine JP, Harrigan J, Hickson ID, Bohr VA. Telomere-binding protein TRF2 binds to and stimulates the Werner and Bloom syndrome helicases. J Biol Chem. 2002; 277:41110–41119. [PubMed: 12181313]

Parrinello S, Coppe JP, Krtolica A, Campisi J. Stromal-epithelial interactions in aging and cancer: senescent fibroblasts alter epithelial cell differentiation. J Cell Sci. 2005; 118:485–496. [PubMed: 15657080]

Pignolo RJ, Suda RK, McMillan EA, Shen J, Lee SH, Choi Y, Wright AC, Johnson FB. Defects in telomere maintenance molecules impair osteoblast differentiation and promote osteoporosis. Aging Cell. 2008; 7:23–31. [PubMed: 18028256]

Potier E, Ferreira E, Andriamanalijaona R, Pujol JP, Oudina K, Logeart-Avramoglou D, Petite H. Hypoxia affects mesenchymal stromal cell osteogenic differentiation and angiogenic factor expression. Bone. 2007; 40:1078–1087. [PubMed: 17276151]

Saeed H, Abdallah BM, Ditzel N, Catala-Lehnen P, Qiu W, Amling M, Kassem M. Telomerase-deficient mice exhibit bone loss owing to defects in osteoblasts and increased osteoclastogenesis by inflammatory microenvironment. J Bone Miner Res. 2011; 26:1494–1505. [PubMed: 21308778]

Salim A, Nacamuli RP, Morgan EF, Giaccia AJ, Longaker MT. Transient changes in oxygen tension inhibit osteogenic differentiation and Runx2 expression in osteoblasts. J Biol Chem. 2004; 279:40007–40016. [PubMed: 15263007]

Shi S, Gronthos S, Chen S, Reddi A, Counter CM, Robey PG, Wang CY. Bone formation by human postnatal bone marrow stromal stem cells is enhanced by telomerase expression. Nat Biotechnol. 2002; 20:587–591. [PubMed: 12042862]

Simonsen JL, Rosada C, Serakinci N, Justesen J, Stenderup K, Rattan SI, Jensen TG, Kassem M. Telomerase expression extends the proliferative life-span and maintains the osteogenic potential of human bone marrow stromal cells. Nat Biotechnol. 2002; 20:592–596. [PubMed: 12042863]

Urushibara A, Kodama S, Suzuki K, Desa MB, Suzuki F, Tsutsui T, Watanabe M. Involvement of telomere dysfunction in the induction of genomic instability by radiation in scid mouse cells. Biochem Biophys Res Commun. 2004; 313:1037–1043. [PubMed: 14706647]

Wang X, Kua HY, Hu Y, Guo K, Zeng Q, Wu Q, Ng HH, Karsenty G, de Crombrugghe B, Yeh J, Li B. p53 functions as a negative regulator of osteoblastogenesis, osteoblast-dependent osteoclastogenesis, and bone remodeling. J Cell Biol. 2006; 172:115–125. [PubMed: 16380437]

Yankiwski V, Marciniak RA, Guarente L, Neff NF. Nuclear structure in normal and Bloom syndrome cells. Proc Natl Acad Sci U S A. 2000; 97:5214–5219. [PubMed: 10779560]

Yudoh K, Matsuno H, Nakazawa F, Katayama R, Kimura T. Reconstituting telomerase activity using the telomerase catalytic subunit prevents the telomere shorting and replicative senescence in human osteoblasts. J Bone Miner Res. 2001; 16:1453–1464. [PubMed: 11499868]

Zaccagnini G, Gaetano C, Della Pietra L, Nanni S, Grasselli A, Mangoni A, Benvenuto R, Fabrizi M, Truffa S, Germani A, Moretti F, Pontecorvi A, Sacchi A, Bacchetti S, Capogrossi MC, Farsetti A. Telomerase mediates vascular endothelial growth factor-dependent responsiveness in a rat model of hind limb ischemia. J Biol Chem. 2005; 280:14790–14798. [PubMed: 15687494]

Zhou S, Greenberger JS, Epperly MW, Goff JP, Adler C, Leboff MS, Glowacki J. Age-related intrinsic changes in human bone-marrow-derived mesenchymal stem cells and their differentiation to osteoblasts. Aging Cell. 2008; 7:335–343. [PubMed: 18248663]

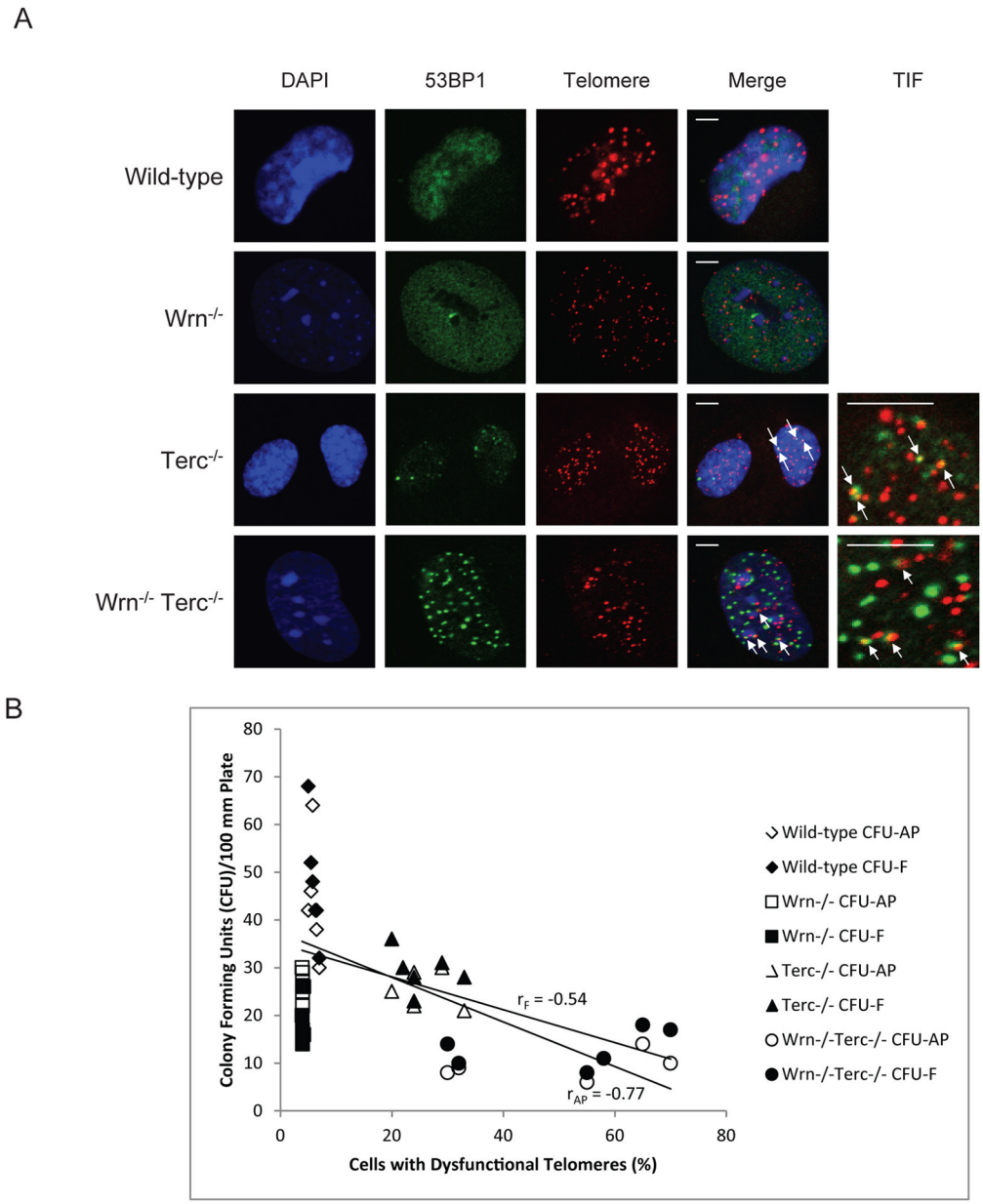

Figure 1.

Telomere dysfunction-induced foci (TIFs) are abundant in MPCs derived from $Terc^{-/-}$ and $Wrn^{-/-}Terc^{-/-}$ mutant mice (A). Co-localizion of 53BP1 DNA damage protein and telomeric DNA. TIFs are indicated by arrows. Blue, DAPI; Green; 53BP1; Red, Telomere; Orange/Yellow; TIF. Scale bar presents 5 μm. (B) Telomere dysfunction correlates with MPC number and osteoblast differentiation.

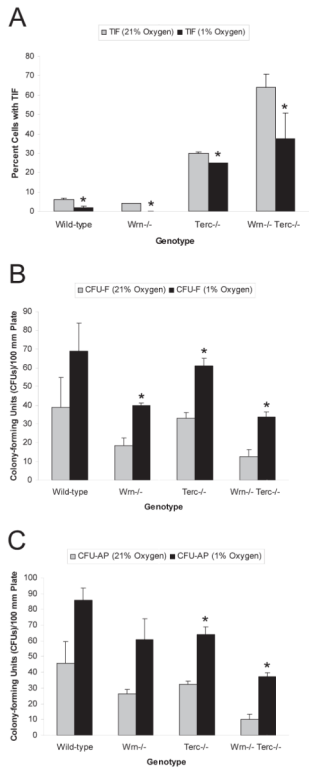

Figure 2.

Reduction in genotoxic stress by lowering of oxygen tension improves telomere maintenance and normalizes MPC number as well as osteoblast differentiation. Low oxygen decreases the number of TIFs across all genotypes (A), increases the number of CFU-F across all mutant genotypes (B), and the number of CFU-AP in $Terc^{-/-}$ and $Wrn^{-/-}$ $Terc^{-/-}$ mutants (C). *, statistically significant compared to 21% O_2 ($p < 0.05$); CFU, colony forming unit; F, fibroblast; AP, alkaline phosphatase.

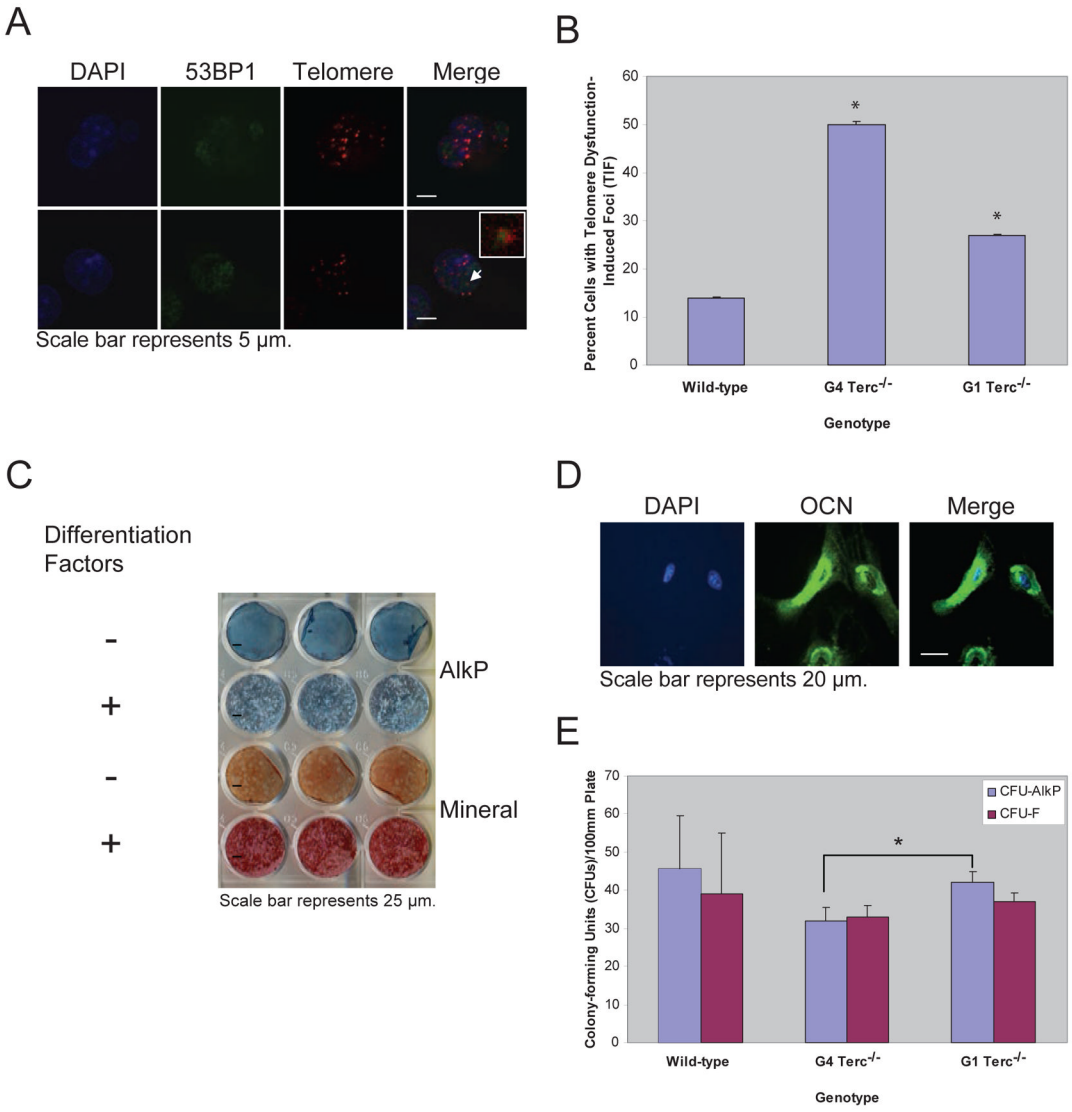

Figure 3.

Limiting telomeric attrition preserves MPC number and osteoblast differentiation in Terc$^{-/-}$ mice. Effects of limited telomere attrition on the number of TIFs (A, B) and concomitant measures of osteoblast differentiation (C–E) in MPCs derived from G4 and G1 Terc$^{-/-}$ animals. Alk P, alkaline phosphatase; Mineral, mineralization; OCN, osteocalcin; colony-forming unit-fibroblast, CFU-F; colony-forming unit-Alk P (CFU-AP). *, statistically significant ($p < 0.05$).

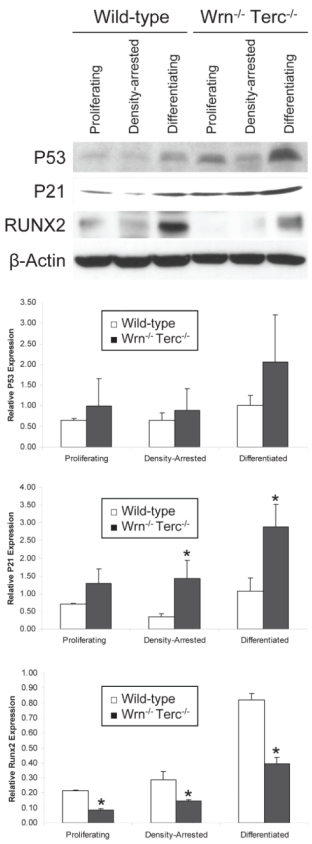

Figure 4.

Enhanced p53/p21 signaling with osteoblast differentiation in $Wrn^{-/-}Terc^{-/-}$animals. Western blot analysis of p53, p21, and RUNX2 in MPCs derived from wild-type and $Wrn^{-/-}Terc^{-/-}$ mutant mice under the given conditions (left). Quantification of the indicated proteins relative to β-actin (right). *, statistically significant ($p < 0.05$).

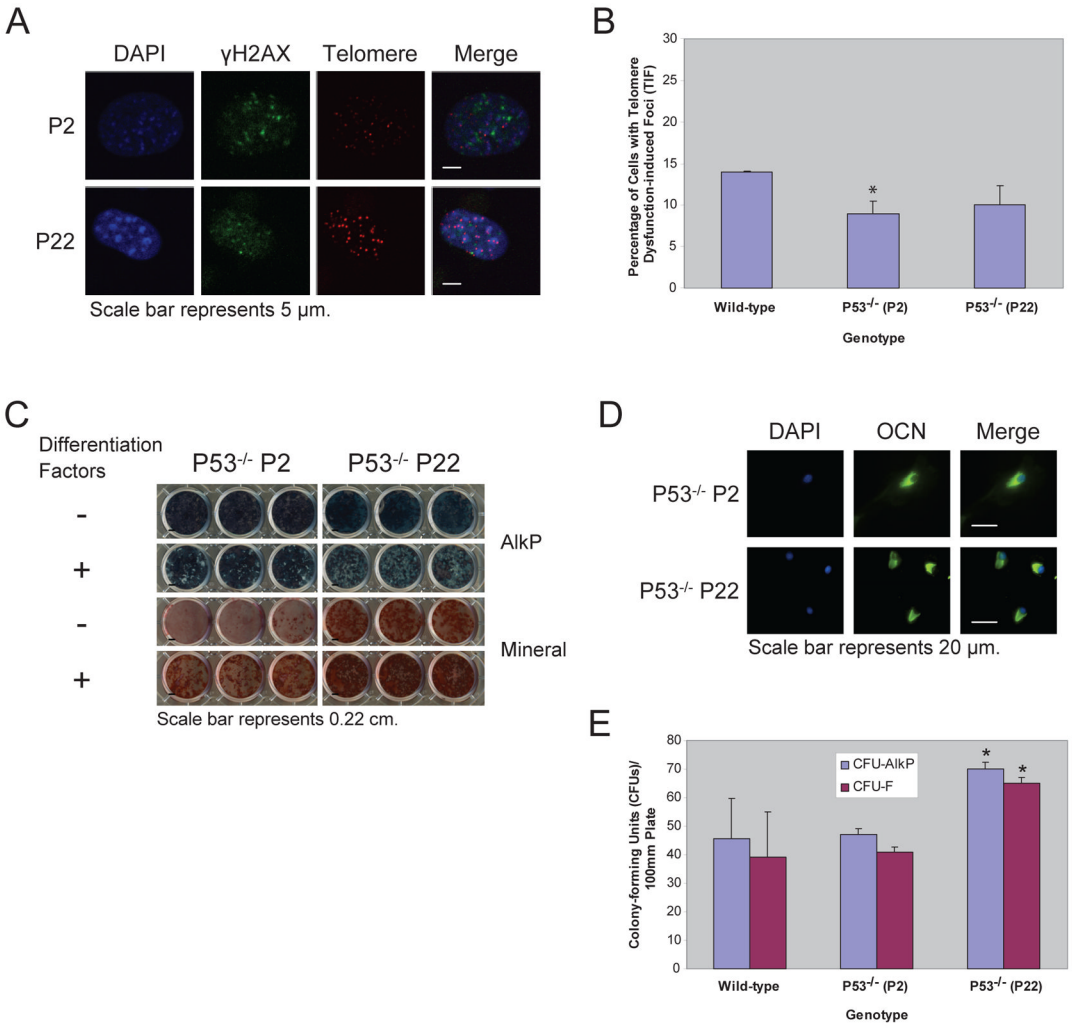

Figure 5.

MPCs from $p53^{-/-}$ mice display minimal telomere dysfunction and undergo spontaneous osteoblast differentiation. TIF+ MPCs from $p53^{-/-}$ animals are compared to wild-type (A, B). Osteoblast differentiation is shown, as measured by alkaline phosphatase activity, mineralization, and osteocalcin expression in $p53^{-/-}$ MPCs (C, D). The numbers of CFU-F and CFU-Alk P in $p53^{-/-}$ MPCs are compared to wild-type (E). Alk P, alkaline phosphatase; Mineral, mineralization; OCN, osteocalcin; colony-forming unit-fibroblast, CFU-F; colony-forming unit-Alk P (CFU-AP). *, statistically significant ($p < 0.05$).

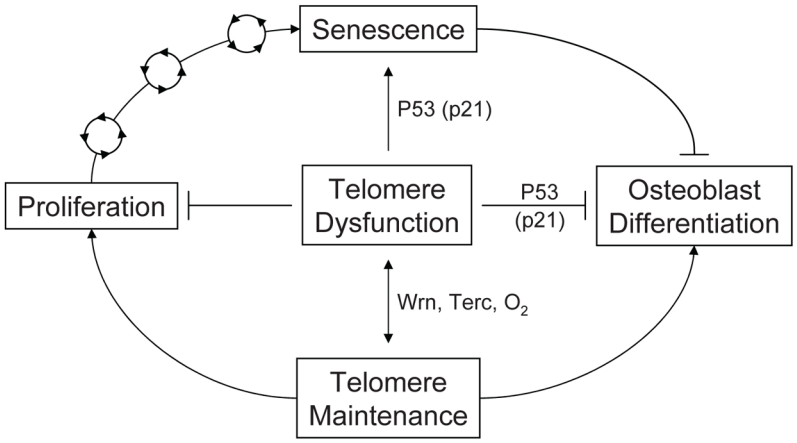

Figure 6.

Model depicting the relationships among telomere dysfunction/maintenance and proliferation, senescence, and osteoblast differentiation. Osteoblast differentiation is impaired by telomere dysfunction independent of proliferation. ⊤, inhibition; →, direct relationship; ↔, reciprocal relationship.